Conductivity of a semi-infinite electron gas: Effective "optical" surface region

Ruben G. Barrera
Institute of Physics, University of Mexico, Mexico 20, D. F., Mexico

Amitabha Bagchi
Department of Physics and Astronomy, University of Maryland, College Park, Maryland 20742

(Received 13 November 1978)

The nonlocal conductivity tensor for a semi-infinite electron gas bounded by a finite-step potential is studied, both numerically and analytically, within the random-phase approximation. The tensor component normal to the surface is compared with the corresponding nonlocal conductivity tensor of the bulk, or homogeneous, electron gas with a view to isolating the "optical" surface region, i.e., the region near the surface in which the two functions differ. It is shown that the slow asymptotic decay of the two functions makes it impossible to define an unambiguous optical surface region at low frequencies below the photoemission threshold. It is also shown by direct numerical comparison that the width of the surface region is strongly frequency dependent. The significance of these conclusions in terms of theoretical approaches to the study of optical reflectance from metal surfaces is discussed.

I. INTRODUCTION

The present interest in the dynamical behavior of electrons close to the surface of a metal together with the recent extensive use of optical probes to study surfaces has stimulated interest in detailed calculations of the electromagnetic field associated with the reflection and refraction of light at a metal surface. Several of these calculations use the concept of a surface region, and it is the purpose of this paper to discuss its meaning through the analysis of a particular model.

The existence of a surface region in the calculation of the reflection coefficient was originally considered by Drude.[1] This region was defined as a transition layer where the local dielectric function varied continuously from its bulk value on one side of the interface to its bulk value on the other side of it. In a local model this will also be the region where the local electron density varies correspondingly. Drude's results can be obtained by considering the transition layer as characterized by the average value of the local dielectric function in this region. An application of these results to reflection spectroscopy from adsorbate layers leads directly to the formulas given by McIntyre and Aspnes.[2]

The determination of a surface region when a nonlocal dielectric function is used to characterize the system is a more complicated and rather enduring problem. Pippard[3] was the first one to point out the importance of the nonlocal nature of the electrical conductivity in his treatment of the anomalous skin effect. This problem was solved later by Reuter and Sondheimer[4] through the solution of the Boltzmann equation in the relaxation-time approximation. They obtained exact expressions for the fields associated with electromagnetic waves in a metal by assuming specular reflection of electrons at the surface and normal incidence of light. It was also remarked[5] that for this model and in a certain range of frequencies, wavelike solutions do not exist in the bulk and only the inclusion of the surface leads to well-behaved results. This means that in this frequency range the solutions in the metal are true surface excitations; in other words, that the surface region is of infinite extent.

The microscopic theory of reflection of *p*-polarized light from a semi-infinite electron gas was worked out by Kliewer and Fuchs.[6] They assumed that the local electron density is uniform and terminates sharply at the surface of the metal, and that the electrons are specularly reflected from it, the so called semi-classical infinite-barrier model (SCIB). Since *p*-polarized light is able to induce charge fluctuations in the system the main difference between this theory and the theory of reflection of *s*-polarized light is that for *p*-polarized light the reflectance as a function of frequency shows structure close to the plasma frequency. The nonlocality was treated both classically through the solution of the Boltzmann equation and quantum mechanically through the introduction of the bulk nonlocal dielectric function. Attempts were also subsequently made to take into account electron lifetime effects in the Lindhard expression for the dielectric function[7,8] as well as diffusive electron scattering from the surface.[9]

 ©1979 The American Physical Society

For the SCIB model a closed-form expression for the electric field inside the metal for p-polarized light has been discussed recently,[10,11] and detailed calculations[12] show that it approaches its bulk value as $1/z^2$ where z is the distance from the surface. This allows us to distinguish between an "optical" surface region, defined as a region beyond which the electric field assumes its bulk value, from a "density" surface region, which is the region over which the local electron density heals to its bulk value. It was in fact pointed out by Apell[12] that in the SCIB model the extent of the optical surface region was much larger than the density surface region, the latter being strictly zero in this case. He also suggested that this feature might persist in a model with a smooth density profile.

A general formalism to calculate the electromagnetic field distribution for the reflection and refraction of light, in the case of more realistic models with smooth electronic density profiles near the surface, has been set up by Feibelman[13] and Mukhopadhyay and Lundqvist.[11] For the calculation of the electric field distribution, both formalisms define a surface region across which the solutions in the vacuum side are matched to those in the metal. In effect the surface region is defined as a region beyond which the dielectric response functions essentially assume their bulk value. This is an alternative, equally acceptable definition of the optical surface region which is the definition we will use in the rest of the paper. Clearly, this too is distinct from the density surface region defined above. Up till now a detailed analysis of the nature and extent of the optical surface region has been lacking. In this paper we try to bridge the gap by explicitly analyzing the behavior of the nonlocal conductivity tensor for a simple quantum-mechanical model of a semi-infinite electron gas.

We consider the electron gas to be bounded by a finite-step potential in the region $z<0$, and translationally invariant in the x-y plane. The conductivity tensor will depend on the x and y variables through the difference while depending on the z coordinates separately. In other words, if effects due to crystallinity can be ignored

$$\vec{\sigma}(\vec{r},\vec{r}';\omega)=\vec{\sigma}(\vec{\rho}-\vec{\rho}',z,z';\omega) \ ,$$

where $\vec{\rho}=\hat{x}x+\hat{y}y$. Effecting a Fourier transformation in the x-y plane, we can describe the system entirely in terms of the Fourier-transformed conductivity[11,13,14] $\vec{\sigma}(\vec{Q},\omega;z,z')$, where $\vec{Q}$ is a wave vector in the x-y plane. It is adequate for most purposes to let $\vec{Q}\to 0$ because wave vectors associated with light are typically much smaller than the Fermi wave vector k_F of electrons. In this paper, we use a combination of numerical and analytical methods to study the spatial dependence of the conductivity tensor within the random-phase approximation (RPA).[14] We look in particular at the zz component, i.e., $\sigma^{zz}(\vec{Q}\to 0,\omega;z,z')$, which is of importance in the interaction of p-polarized light with the metal surface. Our main objective is to determine the optical surface region, i.e., the distance $|\xi|$ such that for $z,z'<\xi$ $(\xi<0)$, $\sigma^{zz}(0,\omega;z,z')\to\sigma_0^{zz}(0,\omega;z,z')$, where the conductivity-tensor component with the subscript 0 refers to a uniform electron gas having the same electron density as in the bulk of the metal. Our procedure here is to make an explicit determination of the optical surface region by *directly* comparing the conductivity tensors σ^{zz} and σ_0^{zz} as a function of position for various frequencies. We find that within the RPA and ignoring electronic lifetime effects, the two functions approach each other asymptotically as one goes into the metal; but the approach is rather slow, and the width of the surface region turns out to be strongly frequency dependent. Furthermore, as has been pointed out already,[12] the optical surface region is indeed larger than the density surface region. We find this to be especially true for photon frequencies below the threshold for photoemission, where it is impossible to determine an optical surface region unambiguously. In the high-frequency or photoemission regime, however, the conductivity tensor approaches its bulk value more rapidly, and an optical surface region can be defined with greater confidence. We conclude that below the photoemission threshold, where surface reflectance spectroscopy[15,16] can be used, it is preferable to formulate a theory of reflection which does not depend explicitly on isolating a particular surface region.[17,18]

Since our results do not include a finite electron lifetime, we would like to point out that the semiclassical calculation of Reuter and Sondheimer[4] has shown that the range of nonlocality of the electrical conductivity is governed by the electron mean free path at low frequencies, but at high frequencies it is governed by the distance traveled by an electron during one complete oscillation of the electric field, irrespective of the electron lifetime. Therefore the argument of Melnyk and Harrison[19] that the metal response is bulklike beyond an electron mean free path is open to question although it might be valid in the low-frequency regime. In fact, our quantum-mechanical calculations for infinite electron lifetimes show a frequency-dependent optical surface region beyond which the range of nonlocality is essentially governed by the singularities of Lindhard's dielectric function.[20] The inclusion of a finite electron lifetime in our model might be the subject of further investigation.

The organization of the paper is as follows. In Sec. II we present our results for the RPA conductivity in the homogeneous electron gas for various frequencies. Particular emphasis is placed on the long-range characteristics of $\sigma_0^{zz}(0,\omega;z,z')$, including oscillations and decay, as $z-z'$ becomes large. In Sec. III we first introduce our model of a semi-infinite electron

gas confined by a finite-barrier step potential. We select out several values of ω, and for a given frequency, we compare the conductivity-tensor components σ^{zz} and σ_0^{zz} as functions of z' for various choices of z. The comparison of these two functions allows us to draw conclusions about the length $|\xi|$ of the optical surface region. In this section, we also go analytically to the limit of an infinite barrier and make contact with previous theoretical work.[11] Section IV summarizes our conclusion and critically evaluates some ideas for further study. Certain details of our calculation of the conductivity-tensor components are contained in the Appendix.

II. RANDOM-PHASE APPROXIMATION IN BULK JELLIUM

The general form of the nonlocal conductivity tensor in the RPA, for an electron gas which is uniform in the x-y plane, has been derived by previous authors.[11,13,14] Adopting the notation of Ref. 14, the zz component of the tensor is given by

$$\sigma^{zz}(0,\omega;z,z') = \frac{ie^2 n(z)}{m\omega}\delta(z-z') + \frac{2i}{\omega}\left[\frac{e\hbar}{2mi}\right]^2 \int \frac{d^2K}{(2\pi)^2} \sum_{\kappa\kappa'} \frac{f(\epsilon_{\vec{K}\kappa}) - f(\epsilon_{\vec{K}\kappa'})}{\hbar\omega + i\eta + \epsilon_\kappa - \epsilon_{\kappa'}} j_{\kappa\kappa'}(z) j_{\kappa'\kappa}(z') \quad , \tag{1}$$

where $\epsilon_{\vec{K}\kappa} (= \hbar^2 K^2/2m + \epsilon_\kappa)$ is the energy of an electron in a state given by $\psi_{\vec{K}\kappa}(\vec{r}) = e^{i\vec{K}\cdot\vec{\rho}}\phi_\kappa(z)/L$, $f(\epsilon)$ denotes the Fermi occupation function (at $T=0$), $n(z)$ is the electron density on a plane defined by z, and

$$j_{\kappa\kappa'}(z) = \phi_k^*(z)\frac{\partial\phi_{\kappa'}(z)}{\partial z} - \frac{\partial\phi_\kappa^*(z)}{\partial z}\phi_{\kappa'}(z) \quad . \tag{2}$$

For the uniform electron gas in three dimensions, $\phi_\kappa(z) = e^{i\kappa z}/L^{1/2}$, L being the normalization length, and $n(z) \to n_0 = k_F^3/3\pi^2$ where k_F is the Fermi wave vector. Substitution in Eqs. (1) and (2) shows after a little algebra that the δ-function term drops out, and the conductivity-tensor component becomes

$$\begin{aligned}\sigma_0^{zz}(0,\omega;z,z') = \frac{ie^2}{m\omega}\frac{1}{8\pi^2}\Bigg\{ & -i\int_{-k_F}^{k_F} d\kappa\,(k_F^2-\kappa^2)e^{-i\kappa(z-z')} \\ & \times\left[\kappa\left(e^{iq_+(z-z')}\Theta(z-z') - e^{iq_+(z'-z)}\Theta(z'-z)\right) + \left[\frac{\kappa^2+q_+^2}{2q_+}\right]e^{iq_+|z-z'|}\right] \\ & + i\int_{-k_F}^{k_F} d\kappa\,(k_F^2-\kappa^2)e^{i\kappa(z-z')} \\ & \times\left[\kappa\left(e^{-iq_-(z-z')}\Theta(z-z') - e^{-iq_-(z'-z)}\Theta(z'-z)\right) + \left[\frac{\kappa^2+q_-^2}{2q_-}\right]e^{-iq_-|z-z'|}\right]\Bigg\} \quad , \end{aligned} \tag{3}$$

where $q_+ = (\kappa^2+q_m^2)^{1/2}$, $q_m^2 = 2m\omega/\hbar$, and $q_- = (\kappa^2-q_m^2)^{1/2}$ if $\kappa > q_m$ while $q_- = -i(q_m^2-\kappa^2)^{1/2}$ if $\kappa < q_m$. Equation (3) shows that σ_0^{zz} is a function only of $z-z'$. Inspection reveals that the conductivity depends on the magnitude $|z-z'|$ alone. Both these results follow immediately from the translational invariance and reflection symmetry of the uniform electron gas.

It is convenient at this stage to introduce the dimensionless function

$$S_0^{zz}(0,\omega;Z) = \sigma_0^{zz}(0,\omega;Z)/k_F\sigma_b \quad , \tag{4a}$$

where $Z = z-z'$, and $\sigma_b = in_0e^2/m\omega$ is the familiar long-wavelength conductivity of jellium in the random-phase approximation. In fact it is easy to show by direct integration that

$$\sigma_b = \int_{-\infty}^{\infty} dz\,\sigma_0^{zz}(0,\omega;z-z') \quad , \tag{4b}$$

which is the expected result. The dimensionless conductivity tensor of Eq. (4a) can be easily written as a sum of integrals over the dimensionless variable $\mu = \kappa/k_F$. When $q_m < k_F$, we obtain

$$S_0^{zz}(0,\omega;Z) = \tfrac{3}{4}\{[I_1^0(Z) + I_2^0(Z) + I_3^0(Z)] + i[I_4^0(Z) + I_5^0(Z)]\} \quad , \tag{5a}$$

where

$$I_1^0(Z) = -\int_0^1 d\mu\,(1-\mu^2)\left[\mu\sin\mu|\tilde{Z}|\cos\mu_+\tilde{Z} - \left[\frac{\mu^2+\mu_+^2}{2\mu_+}\right]\cos\mu\tilde{Z}\sin\mu_+|\tilde{Z}|\right] \quad , \tag{5b}$$

$$I_2^0(Z) = -\int_0^{\mu_m} d\mu\,(1-\mu^2)\left[\mu\sin\mu|\tilde{Z}| + \left[\frac{\mu^2-\mu_-'^2}{2\mu_-'}\right]\cos\mu\tilde{Z}\right]e^{-\mu_-'|\tilde{Z}|} \quad , \tag{5c}$$

$$I_3^0(Z) = -\int_{\mu_m}^1 d\mu\,(1-\mu^2)\left[\mu\sin\mu|\tilde{Z}|\cos\mu_-\tilde{Z} - \left(\frac{\mu^2+\mu_-^2}{2\mu_-}\right)\cos\mu\tilde{Z}\sin\mu_-|\tilde{Z}|\right], \tag{5d}$$

$$I_4^0(Z) = -\int_0^1 d\mu\,(1-\mu^2)\left[\mu\sin\mu|\tilde{Z}|\sin\mu_+|\tilde{Z}| + \left(\frac{\mu^2+\mu_+^2}{2\mu_+}\right)\cos\mu\tilde{Z}\cos\mu_+\tilde{Z}\right], \tag{5e}$$

$$I_5^0(Z) = \int_{\mu_m}^1 d\mu\,(1-\mu^2)\left[\mu\sin\mu|\tilde{Z}|\sin\mu_-|\tilde{Z}| + \left(\frac{\mu^2+\mu_-^2}{2\mu_-}\right)\cos\mu\tilde{Z}\cos\mu_-\tilde{Z}\right], \tag{5f}$$

and $\mu_\pm = (\mu^2 \pm \mu_m^2)^{1/2}$, $\mu_-' = (\mu_m^2 - \mu^2)^{1/2}$, while $\mu_m = q_m/k_F = (\hbar\omega/E_F)^{1/2}$, E_F being the Fermi energy. Also $\tilde{Z} = k_F Z = k_F(z-z')$ is a dimensionless length variable. When $q_m > k_F$ (i.e., $\mu_m > 1$), the terms I_3^0 and I_5^0 disappear while the upper limit of the integral for $I_2^0(Z)$ is replaced by unity. We have evaluated S_0^{zz} numerically by performing the integrations using Simpson's rule. Figure 1 shows the real and imaginary parts of $S_0^{zz}(0,\omega;z-z')$ plotted against

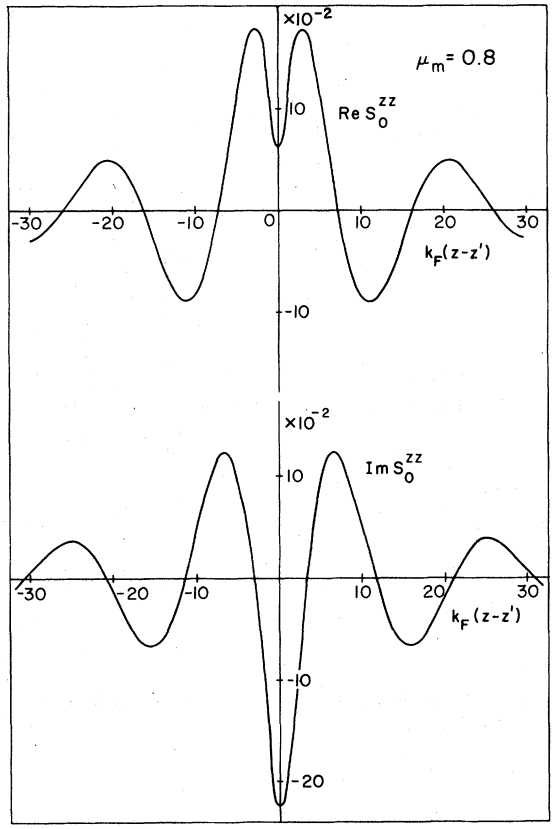

FIG. 1. Real and imaginary parts of $S_0^{zz}(0,\omega;z-z')$, the dimensionless nonlocal conductivity function of a free-electron gas as defined in Eq. (4) of the text, plotted against $k_F(z-z')$. Frequency of light is denoted by the parameter $\mu_m = (\hbar\omega/E_F)^{1/2}$, where E_F and k_F are the Fermi energy and the Fermi momentum, respectively.

$k_F(z-z')$ for $\mu_m = 0.8$, i.e., $\hbar\omega = 0.64E_F$. As expected, the functions are symmetric, and they oscillate and decay slowly as $|z-z'|$ increases. These oscillations are not the usual, static Friedel oscillations but are rather their dynamical counterparts as we shall explain below. The length of decay is, of course, a measure of the range of nonlocality of the conductivity function.

In order to obtain physical insight into the behavior of these functions, especially in the asymptotic region, we note that $\sigma_0^{zz}(0,\omega;Z)$ may be regarded as a one-dimensional Fourier transform of the longitudinal conductivity function $\sigma_{\parallel}(\vec{q}=q\hat{z},\omega)$ of Lindhard[20] for the free-electron gas. Since the real (dissipative) part of $\sigma_{\parallel}(\vec{Q},\omega)$ is necessarily positive, it follows that the real part of $\sigma_0^{zz}(0,\omega;Z)$ must be positive when $Z=0$. This expectation is borne out in Fig. 1 once we recognize that Eq. (4a) may be recast as

$$\sigma_0^{zz}(0,\omega;Z) = k_F\frac{n_0e^2}{m\omega}\left[-\mathrm{Im}S_0^{zz}(0,\omega;Z) + i\,\mathrm{Re}S_0^{zz}(0,\omega;Z)\right]. \tag{6}$$

Furthermore, the asymptotic ($|Z|\to\infty$) behavior of $\sigma_0^{zz}(0,\omega;Z)$ is known to be controlled[21] by the singularity structure of the Fourier transform function $\sigma_{\parallel}(\vec{q},\omega)$. The singularities of the latter are of the type[20]

$$(q-q_i)\ln|q-q_i|\ ,$$

where q_i's are solutions of the equation

$$\hbar\omega \pm \hbar^2q_i^2/2m \pm \hbar^2q_ik_F/m = 0\ . \tag{7a}$$

In other words,

$$q_i = \pm k_F \pm (k_F^2 \mp 2m\omega/\hbar)^{1/2}\ . \tag{7b}$$

The longest wavelength oscillations come from the smallest q_i, viz., $q_i = q_s = (k_F^2+q_m^2)^{1/2} - k_F$ with $q_m = (2m\omega/\hbar)^{1/2}$, and this wave vector increases and the corresponding wavelength of oscillations of σ_0^{zz} in real space decreases as the frequency ω goes higher. This feature is evident in Fig. 2 where we have plotted the real and imaginary parts of $S_0^{zz}(0,\omega;z-z')$ vs $k_F|z-z'|$ for a range of values of μ_m lying between

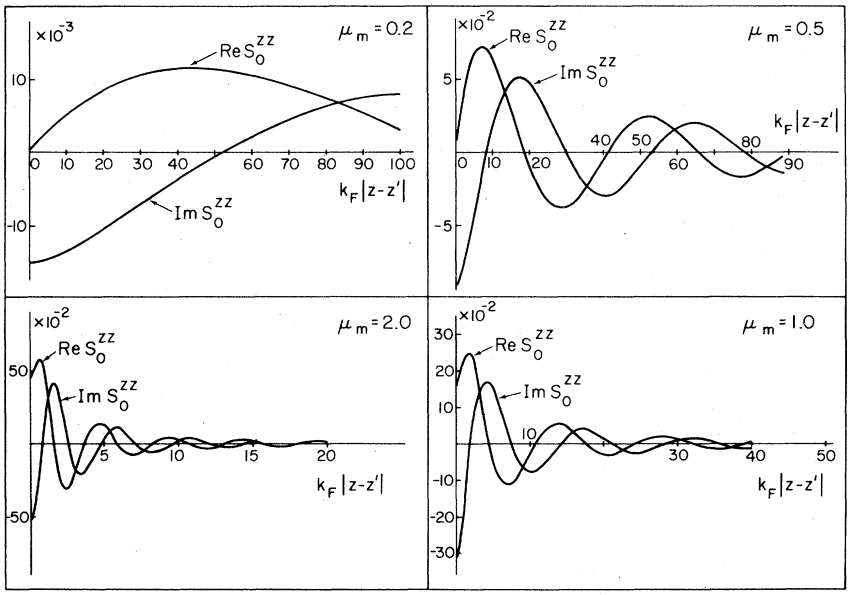

FIG. 2. Real and imaginary parts of the dimensionless, nonlocal conductivity function $S_0^{zz}(0,\omega;z-z')$ of the homogeneous electron gas, plotted against $k_F|z-z'|$, for a range of frequencies denoted by the value of $\mu_m=(\hbar\omega/E_F)^{1/2}$ in each panel. The functions are symmetric in the argument $z-z'$.

0.2 and 2.0. Superimposed on these oscillations, although not visible in the figure, are oscillations of much smaller wavelengths which, as Eq. (7b) shows, go over to the usual Friedel oscillations of wave vector $2k_F$ in the static limit ($\omega=0$). The singularity structure of $\sigma_{\parallel}(\vec{q},\omega)$ also ensures[21] that $S_0^{zz}(0,\omega;Z)$ falls off asymptotically as $|Z|^{-2}$. This slow falloff, which has been pointed out earlier,[11] is exhibited by the curves of Fig. 2.

A feature of the spatial dependence of $\sigma_0^{zz}(0,\omega;z-z')$, which is of interest and worth pointing out, is that the range of nonlocality of the function is quite large, in units of k_F^{-1}, although the range decreases as the frequency ω is increased. We turn now to a comparison of the conductivity tensor of the uniform electron gas with that of a semi-infinite system.

III. RPA IN SEMI-INFINITE JELLIUM WITH FINITE BARRIER

A. Numerical

To construct the model for a metal which is translationally invariant parallel to its surface, we consider a semi-infinite electron gas confined to $z<0$ by means of the step potential $V(\vec{r})=-V_0\Theta(-z)$. We choose $V_0=10.7$ eV, and assume that the metal has a work function $\phi=4.5$ eV. This implies that the Fermi energy is $E_F=6.2$ eV, which corresponds to an r_s value of 2.92 and $k_F\cong 1.27$ Å^{-1}. The wave functions in the potential are exactly known, and hence the electron density near the surface is easily calculated. We find that the actual electron density $n(z)$ differs from the bulk density n_0 by less than one percent by the time $k_Fz\lesssim -7.5$. This distance may then be taken as a measure of the density surface region. The conductivity-tensor component $\sigma^{zz}(0,\omega;z,z')$ now depends on z and z' separately, rather than simply on $z-z'$. Let us, once again, define the dimensionless, nonlocal function

$$S^{zz}(0,\omega;z,z')=\sigma^{zz}(0,\omega;z,z')/k_F\sigma_b \ . \tag{8}$$

As shown in the Appendix, this function may be written as a sum of integrals $I_i(z,z')$ $[i=1,\ldots,5]$. Inside the metal ($z,z'<0$), these integrals are of the same type as $I_i^0(z-z')$ of Eqs. (5a)–(5f), but the integrands are considerably more complicated. The integrals can be evaluated using Simpson's rule. The numerical calculation, however, becomes time consuming for large and negative values of z and z' because of the presence of oscillatory terms in the integrands.

To show the results of our computation for the conductivity tensor, we first choose a photon energy of $\hbar\omega=4.0$ eV which corresponds to $\mu_m=0.803$. This photon energy is below the threshold for photoemission, and is a typical one used in studies on surface reflectance.[15,16] We select a set of values of z, and for each z, compute $S^{zz}(0,\omega;z,z')$ as a function of z'. Figure 3 shows the real part of $S^{zz}(0,\omega;z,z')$ as a function of z' for several values of z inside the metal

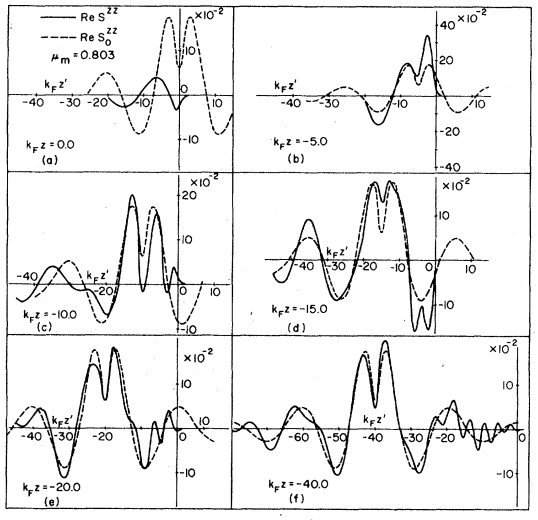

FIG. 3. Real part of the dimensionless, nonlocal conductivity function $S^{zz}(0, \omega; z, z')$ of a semi-infinite electron gas, confined to the region $z < 0$ by means of a step potential of magnitude $V_0 = 10.7$ eV, shown as full lines plotted against $k_F z'$ for a range of values of z: (a) $z = 0.0$, (b) $z = -5k_F^{-1}$, (c) $z = -10k_F^{-1}$, (d) $z = -15k_F^{-1}$, (e) $z = -20k_F^{-1}$, (f) $z = -40k_F^{-1}$. The graphs are drawn for a photon energy of $\hbar\omega = 4.0$ eV, and the Fermi energy is chosen to be $E_F = 6.2$ eV, corresponding to an r_s value of 2.92. The parameter μ_m stands for $(\hbar\omega/E_F)^{1/2}$. [See Eq. (8) of the text for definition.] The dashed curve in each panel stands for the real part of $S_0^{zz}(0, \omega; z, z')$, the dimensionless conductivity appropriate to the uniform electron gas. The latter function depends only on the magnitude of the difference $z - z'$.

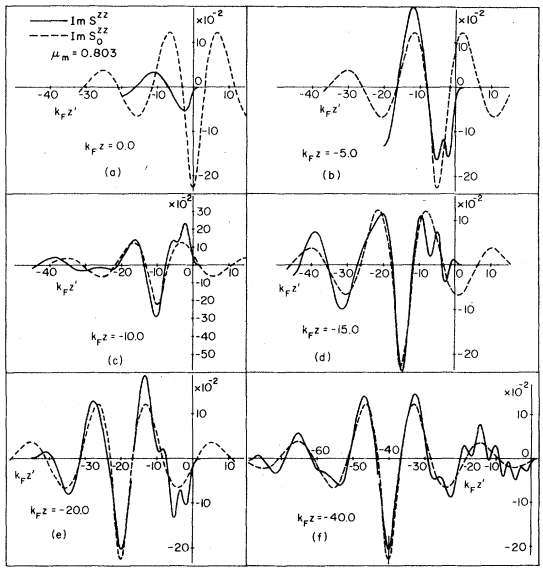

FIG. 4. Imaginary part of the dimensionless, nonlocal conductivity function $S^{zz}(0, \omega; z, z')$ of a semi-infinite electron gas bounded by the potential $V(\vec{r}) = -V_0\Theta(-z)$ with $V_0 = 10.7$ eV, shown as full curves when plotted vs $k_F z'$ for a range of values of z: (a) $z = 0.0$, (b) $z = -5k_F^{-1}$, (c) $z = -10k_F^{-1}$, (d) $z = -15k_F^{-1}$, (e) $z = -20k_F^{-1}$, (f) $z = -40k_F^{-1}$. The light frequency and Fermi energy used in the numerical calculations are given in the caption to Fig. 3. The dashed curve in each panel represents the imaginary part of $S_0^{zz}(0, \omega; |z - z'|)$, the dimensionless conductivity function appropriate to the bulk, i.e., homogeneous, electron gas.

$(z < 0)$. For purposes of comparison, we have also plotted the uniform-electron-gas conductivity $\mathrm{Re}[S_0^{zz}(0, \omega; z, z')]$, which is, naturally, independent of z, as a dashed curve in each panel. We have taken z to range between 0 and -40 (in units of k_F^{-1}). A similar comparison of the imaginary parts of S^{zz} and S_0^{zz} as functions of z' for selected values of z is shown in Fig. 4.

From a study of Figs. 3 and 4, it appears that the conductivity tensor for the semi-infinite metal does indeed approach its bulk counterpart as one goes into the metal. But the convergence is rather slow, at least at $\mu_m = 0.803$. At this frequency, differences in the conductivity of the semi-infinite metal and the uniform electron gas seemingly persist as we go into the bulk of the metal $(z' < z)$ even for $k_F z = -40$. On the other hand, as we approach the surface $(z < z' \to 0)$, the conductivity in the semi-infinite case shows rapid oscillations. These rapid oscillations arise from quantum-mechanical interference effects owing to the presence of the surface, and are naturally absent in the uniform electron system. It is safe to conclude that at this frequency, the optical surface region has an extent $|\xi| \gtrsim 40k_F^{-1}$. Later on in this section, we shall try to make more precise the criterion for determining the length $|\xi|$.

As the frequency ω is increased, we find that the functions $S^{zz}(0, \omega; z, z')$ and $S_0^{zz}(0, \omega; z, z')$ converge more rapidly for $z' < z$ as z goes into the metal. Since the range of nonlocality also decreases with frequency, and the quantum-mechanical interference effects become much less pronounced, the functions appear to converge for $z' > z$ as well. The point is made clearly in Fig. 5 where we have plotted the real and imaginary parts of $S^{zz}(0, \omega; z, z')$ as functions of z' for two choices of z, viz., $k_F z = -5.0$ and -20.0, with a photon energy in the photoemission regime, viz., $\mu_m = 2\hbar\omega = 4E_F = 24.8$ eV. For comparison purposes, we have also shown the real and imaginary parts of $S_0^{zz}(0, \omega; z - z')$ on the same figure. The conductivity curves for $z = -20k_F^{-1}$ are very close to (but not identical with) the curves for the uniform electron gas over the relevant range of nonlocality. The agreement between S^{zz} and S_0^{zz} is even better at $k_F = -20$ at higher frequency, as is shown in Fig. 6 where we have chosen $\mu_m = 3$ so that

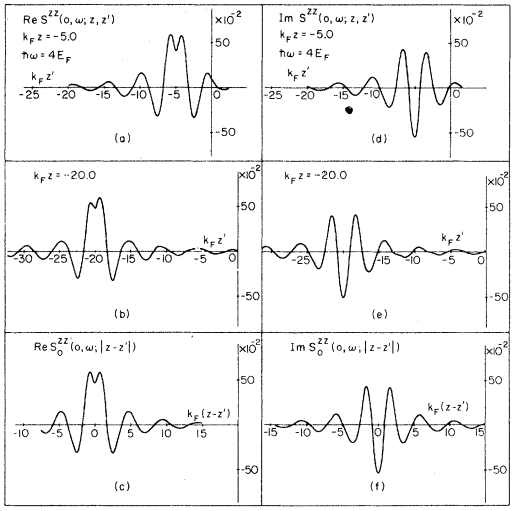

FIG. 5. Real parts [curves (a) and (b)] and the imaginary parts [curves (d) and (e)] of $S^{zz}(0,\omega;z,z')$ shown against $k_F z'$ for two values of z, viz., $z=-5k_F^{-1}$ in curves (a) and (d), and $z=-20k_F^{-1}$ in curves (b) and (e), for the choice $\hbar\omega=4E_F$. The parameters of the model are indicated in the caption to Fig. 3. For comparison purposes, panels (c) and (f) show, respectively, the real and imaginary parts of the function $S_0^{zz}(0,\omega;|z-z'|)$. See Eq. (4a) and (8) of the text for definitions.

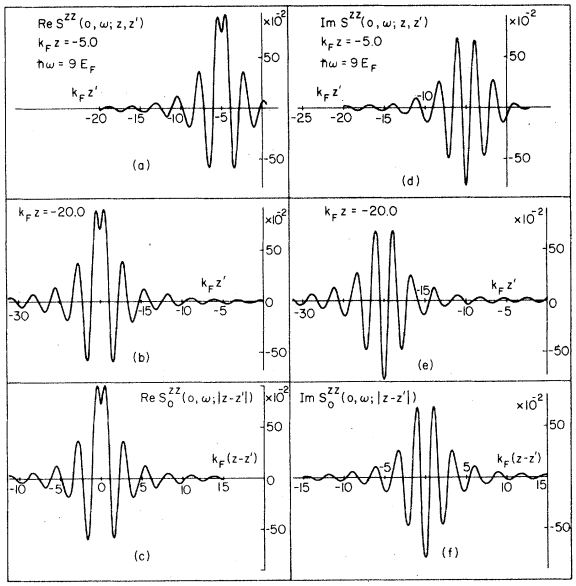

FIG. 6. Real parts [curves (a) and (b)] and the imaginary parts [curves (d) and (e)] of $S^{zz}(0,\omega;z,z')$ shown against $k_F z'$ for two values of z, viz., $z=-5k_F^{-1}$ in curves (a) and (d), and $z=-20k_F^{-1}$ in curves (b) and (e), for the choice $\hbar\omega=9E_F$. The parameters of the semi-infinite electron gas are given in the caption to Fig. 3. For comparison purposes, panels (c) and (f) show the real and imaginary parts, respectively, of $S_0^{zz}(0,\omega;|z-z'|)$, the conductivity function for the uniform electron gas. See Eqs. (4a) and (8) of the text for definitions.

$\hbar\omega=9E_F=55.8$ eV.

The most obvious conclusion to be drawn from Figs. 3–6 is that the optical surface region $|\xi|$, insofar as it can be defined, depends strongly on the frequency of light. It is also clear that this distance is, in general, larger than the distance over which the electron density near the surface heals to its bulk value.[22] To make our conclusions sharper, we must devise criteria for determining the length $|\xi|$. This is what we now proceed to do.

B. Analytical

A plausible definition of the extent of the optical surface region, which depends only on the response functions of the system, is that it is the length $|\xi|$ such that for all z and $z'<\xi$,

$$|S^{zz}(0,\omega;z,z')-S_0^{zz}(0,\omega;z-z')|<\epsilon\ , \tag{9}$$

where ϵ is an arbitrary but predetermined small number. Our numerical calculations show that the functions S^{zz} and S_0^{zz} do approach each other asymptotically as $z,z'\to-\infty$. Hence the above criterion can lead to a meaningful definition of the length $|\xi|$, especially for high-photon energies above the threshold of photoemission, as is illustrated by Figs. 5 and 6. Below the photoemission threshold, however, the situation is more complicated. For example, Figs. 3 and 4 seem to indicate that in this frequency region, even though the difference between S^{zz} and S_0^{zz} tends to zero for a given z (<0) as $z'\to-\infty$, the difference has the same order of magnitude as the functions themselves. Such a behavior is characteristic of a power-law decay of the individual, nonlocal conductivity functions. As was pointed out in Sec. II, the dimensionless conductivity tensor for the homogeneous system, i.e., $S_0^{zz}(0,\omega;|Z|)$, has the asymptotic behavior (apart from oscillatory terms) of $|Z|^{-2}$ as $|Z|\to\infty$. The asymptotic behavior of S^{zz} can be explicitly studied in the limit of the semi-classical infinite-barrier model.[11] This limit is defined by letting $V_0\to\infty$ and ignoring the quantum-mechanical interference effects. As shown in the Appendix, this yields

$$S^{zz}(0,\omega;z,z')\underset{z,z'<0}{=}S_0^{zz}(0,\omega;|z-z'|)-S_0^{zz}(0,\omega;|z+z'|)\ . \tag{10}$$

Clearly a power-law decay of S^{zz} is dictated by the

above equation for a fixed z and $(z-z') \to \infty$. This feature prevents us from arriving at an unambiguous length scale $|\xi|$, based on the criterion of Eq. (9) for the optical surface region. In fact, combining Eqs. (9) and (10), one finds that the criterion for finding $|\xi|$ is now

$$|S^{zz}(0,\omega;z,z') - S_0^{zz}(0,\omega;|z-z'|)| = |S_0^{zz}(0,\omega;|z+z'|)| < \epsilon \ , \quad (11)$$

when $z,z' < \xi$. Since $|z+z'| > 2|\xi|$ for $z,z' < \xi$, one can always find a ξ for a given ϵ to meet the above criterion. Such a length scale $|\xi|$, however, will be strongly ϵ dependent, going as a power of $1/\epsilon$. Consequently it would be impossible to assign an unambiguous optical surface region to the semiclassical infinite-barrier model. Since the curves for S^{zz} appearing in Figs. 3 and 4 show qualitatively the same power-law behavior in the asymptotic region, we can extrapolate our argument and conclude that an unambiguous optical surface region cannot be defined in the finite-barrier case also for photon energies below the photoemission threshold. Above the photoemission threshold, the conductivity tensors in RPA still fall off asymptotically as $|z'|^{-2}$ for a fixed z. However the range of nonlocality shrinks rapidly with ω, so that S^{zz} and S_0^{zz} appear to converge quickly over their nonlocality range as z goes into the metal, thus making the definition of the optical surface region less equivocal. It must be pointed out that the inclusion of finite lifetime effects for the excited electrons may allow us to circumvent this uncertainty, as the correlation functions would then fall off exponentially in the asymptotic region $(z-z' \to \infty)$. In that case, the width of the optical surface region based on Eq. (9) would depend only weakly (i.e., logarithmically) on the parameter ϵ.

Another feature of our calculations is that no matter what criterion we choose to adopt for the length of the optical surface region, the results of Figs. 3–6 show conclusively that $|\xi|$ depends on the frequency ω, a fact that has not been discussed before. Since we find that the length is quite large at the frequencies which are of importance in surface reflectance spectroscopy,[15,16] the correction to the usual Fresnel formulas would be more important at lower frequencies. Furthermore the dependence of the optical surface region on ω makes it impossible to isolate a single-surface region (for all ω) across which the solutions to Maxwell's equations ought to be matched. Instead it may be more fruitful to look for solutions to the optical-reflectivity problem not depending explicitly on a consideration of the optical surface region. A formulation of the problem along these lines has been reported recently.[18]

IV. CONCLUSIONS

We study in this paper a particular (i.e., zz) component of the nonlocal conductivity tensor of a semi-infinite electron gas within the RPA without electronic lifetime effects. We compare the conductivity function of the semi-infinite problem with the corresponding function for the uniform electron gas within the same approximation. Our aim is to determine the optical surface region which is defined as the distance into the metal beyond which the conductivity functions would be identical. We find that while the two functions approach each other as we go from the surface of the metal into the bulk, the approach is rather slow at low frequencies, below the photoemission threshold, although it is more rapid at higher frequencies which are of interest in photoemission. We also find that within the approximation studied in this paper, the nonlocal conductivity functions away from the central point $z=z'$ do not approach each other faster than they decay away to zero. Thus the difference between the conductivity functions persist even at large distances, making it difficult to arrive at an unambiguous definition of the optical surface region.

A second point to emerge from our study is that any sensible definition of the optical surface region shows that its length depends sensitively on the frequency of light, as was noted briefly by Mukhopadhyay and Lundqvist.[23] Thus we feel that it is more reasonable to study optical reflectance from a semi-infinite, nonlocal dielectric medium by regarding the surface response as a perturbation on a bulk response function which can be specified on physical grounds without any ambiguity. Such an approach is concerned only with the difference of the conductivity functions σ^{zz} and σ_0^{zz}, and its space integral, so that the need for defining an optical surface region never arises. The solution to the reflectance problem based on this approach has been investigated by us and partly reported.[18]

We finally note that even though our model does not apply to a realistic metallic system, the results we have presented in this paper are important in a limiting sense since they will serve as guides to approximations for the realistic case of an inhomogeneous electron gas including, e.g., lattice effects. Therein lies a major significance of the RPA results for the conductivity tensor discussed here.

ACKNOWLEDGMENTS

The authors wish to acknowledge valuable and informative discussions on various aspects of the problem with Professor R. E. Prange and Professor A. K. Rajagopal. The assistance of A. Mendoza in the numerical calculations is also acknowledged. Sincere

thanks are due to the Computer Centers of the University of Mexico and the University of Maryland for use of their computing facilities. This work was supported in part by NSF under Grant No. DMR 76-82128.

APPENDIX

In this Appendix, we present the formulas for $S^{zz}(0,\omega,z,z')$ used in our numerical calculations. The starting point is Eq. (1), and the wave functions in the finite-barrier potential $V(\vec{r})=-V_0\Theta(-z)$ are exactly known. After a modest amount of algebraic manipulations, it is possible to write it as a sum of single-variable integrals over the Green's functions of the problem for various energies. The integral expressions for the conductivity tensor have different forms in different regions of frequency, viz., $\hbar\omega<\phi$, $\phi<\hbar\omega<E_F$, and $\hbar\omega>E_F$. The expressions are also different in four regions of space, viz., $z,z'<0$; $z<0$, $z'>0$; $z>0$, $z'<0$; and $z,z'>0$. We shall explicitly present our result here below the photoemission threshold ($\hbar\omega<\phi$) for both z and z' lying within the metal. Other frequency regions can be easily reached by appropriate analytic continuation, while similar formulas can be worked out without much difficulty for other regions of space.

Let us define the dimensionless variables $\tilde{z}=k_F z$ and $\tilde{z}'=k_F z'$. For $\hbar\omega<\phi$ and $z,z'<0$, we may write

$$S^{zz}(0,\omega;\tilde{z},\tilde{z}')=\tfrac{3}{4}\{[I_1(\tilde{z},\tilde{z}')+I_2(\tilde{z},\tilde{z}')+I_3(\tilde{z},\tilde{z}')]+i[I_4(\tilde{z},\tilde{z}')+I_5(\tilde{z},\tilde{z}')]\}\ , \tag{A1}$$

where

$$\begin{aligned} I_1(\tilde{z},\tilde{z}')=\int_0^1 d\mu\,(1-\mu^2)\Big\{&-\mu\sin\mu|\tilde{z}-\tilde{z}'|\cos\mu_+(\tilde{z}-\tilde{z}')+\mu\sin[\mu(\tilde{z}+\tilde{z}')+2\delta] \\ &\times[a_1\cos\mu_+(\tilde{z}+\tilde{z}')+a_2\sin\mu_+(\tilde{z}+\tilde{z}')]+\frac{\mu^2}{\mu_+}\cos(\mu\tilde{z}+\delta)\cos(\mu\tilde{z}'+\delta) \\ &\times[\sin\mu_+|\tilde{z}-\tilde{z}'|+a_2\cos\mu_+(\tilde{z}+\tilde{z}')-a_1\sin\mu_+(\tilde{z}+\tilde{z}')]+\mu_+\sin(\mu\tilde{z}+\delta) \\ &\times\sin(\mu\tilde{z}+\delta)[\sin\mu_+|\tilde{z}-\tilde{z}'|-a_2\cos\mu_+(\tilde{z}+\tilde{z}')+a_1\sin\mu_+(\tilde{z}+\tilde{z}')]\Big\}\ , \end{aligned} \tag{A2}$$

$$\begin{aligned} I_2(\tilde{z},\tilde{z}')=\int_0^{\mu_m} d\mu\,(1-\mu^2)\Big\{&-\mu\sin\mu|\tilde{z}-\tilde{z}'|e^{-\mu'_-|\tilde{z}-\tilde{z}'|}+\mu\sin[\mu(\tilde{z}+\tilde{z}')+2\delta]a_3e^{\mu'_-(\tilde{z}+\tilde{z}')} \\ &+\frac{\mu^2}{\mu'_-}\cos(\mu\tilde{z}+\delta)\cos(\mu\tilde{z}'+\delta)\left[\left(\frac{2\mu'^2_-}{\mu_0^2}+1-\frac{2\mu'_-\nu_-}{\mu_0^2}\right)e^{\mu'_-(\tilde{z}+\tilde{z}')}-e^{-\mu'_-|\tilde{z}-\tilde{z}'|}\right] \\ &+\mu'_-\sin(\mu\tilde{z}+\delta)\sin(\mu\tilde{z}'+\delta)(e^{-\mu'_-|\tilde{z}-\tilde{z}'|}-a_3e^{\mu'_-(\tilde{z}+\tilde{z}')})\Big\}\ , \end{aligned} \tag{A3}$$

$$\begin{aligned} I_3(\tilde{z},\tilde{z}')=\int_{\mu_m}^1 d\mu\,(1-\mu^2)\Big\{&-\mu\sin\mu|\tilde{z}-\tilde{z}'|\cos\mu_-(\tilde{z}-\tilde{z}')+\mu\sin[\mu(\tilde{z}+\tilde{z}')+2\delta] \\ &\times[a_4\cos\mu_-(\tilde{z}+\tilde{z}')-a_5\sin\mu_-(\tilde{z}+\tilde{z}')]+\frac{\mu^2}{\mu_-}\cos(\mu\tilde{z}+\delta)\cos(\mu\tilde{z}'+\delta) \\ &\times[\sin\mu_-|\tilde{z}-\tilde{z}'|-a_5\cos\mu_-(\tilde{z}+\tilde{z}')-a_4\sin\mu_-(\tilde{z}+\tilde{z}')]+\mu_-\sin(\mu\tilde{z}+\delta) \\ &\times\sin(\mu\tilde{z}'+\delta)[\sin\mu_-|\tilde{z}-\tilde{z}'|+a_5\cos\mu_-(\tilde{z}+\tilde{z}')+a_4\sin\mu_-(\tilde{z}+\tilde{z}')]\Big\}\ , \end{aligned} \tag{A4}$$

$$I_4(\tilde{z},\tilde{z}') = \int_0^1 d\mu(1-\mu^2)\Big[-\mu\sin\mu(\tilde{z}-\tilde{z}')\sin\mu_+(\tilde{z}-\tilde{z}') + \mu\sin[\mu(\tilde{z}+\tilde{z}')+2\delta]$$
$$\times[a_2\cos\mu_+(\tilde{z}+\tilde{z}') - a_1\sin\mu_+(\tilde{z}+\tilde{z}')] - \frac{\mu^2}{\mu_+}\cos(\mu\tilde{z}+\delta)\cos(\mu\tilde{z}'+\delta)$$
$$\times[\cos\mu_+(\tilde{z}-\tilde{z}') + a_1\cos\mu_+(\tilde{z}+\tilde{z}') + a_2\sin\mu_+(\tilde{z}+\tilde{z}')] - \mu_+\sin(\mu\tilde{z}+\delta)$$
$$\times\sin(\mu\tilde{z}'+\delta)[\cos\mu_+(\tilde{z}-\tilde{z}') - a_1\cos\mu_+(\tilde{z}+\tilde{z}') - a_2\sin\mu_+(\tilde{z}+\tilde{z}')]\Big] , \tag{A5}$$

and

$$I_5(\tilde{z},\tilde{z}') = \int_{\mu_m}^1 d\mu(1-\mu^2)\Big[\mu\sin\mu(\tilde{z}-\tilde{z}')\sin\mu_-(\tilde{z}-\tilde{z}') + \mu\sin[\mu(\tilde{z}+\tilde{z}')+2\delta]$$
$$\times[a_5\cos\mu_-(\tilde{z}+\tilde{z}') + a_4\sin\mu_-(\tilde{z}+\tilde{z}')] + \frac{\mu^2}{\mu_-}\cos(\mu\tilde{z}+\delta)\cos(\mu\tilde{z}'+\delta)$$
$$\times[\cos\mu_-(\tilde{z}-\tilde{z}') + a_4\cos\mu_-(\tilde{z}+\tilde{z}') - a_5\sin\mu_-(\tilde{z}+\tilde{z}')] + \mu_-\sin(\mu\tilde{z}+\delta)$$
$$\times\sin(\mu\tilde{z}'+\delta)[\cos\mu_-(\tilde{z}-\tilde{z}') - a_4\cos\mu_-(\tilde{z}+\tilde{z}') + a_5\sin\mu_-(\tilde{z}+\tilde{z}')]\Big] . \tag{A6}$$

In these expressions, the following definitions have been used:

$$\mu = [(E+V_0)/E_F]^{1/2};\quad \mu_0 = (V_0/E_F)^{1/2};\quad \mu_m = (\hbar\omega/E_F)^{1/2};\quad \mu_\pm^2 = \mu^2 \pm \mu_m^2;\quad \mu_-'^2 = \mu_m^2 - \mu^2;$$
$$\nu = (\mu_0^2-\mu^2)^{1/2};\quad \nu_\pm^2 = \nu^2 \mp \mu_m^2;\quad a_1 = 2\mu_+^2/\mu_0^2 - 1;\quad a_2 = -2\mu_+\nu_+/\mu_0^2;$$
$$a_3 = (\mu_-' - \nu_-)/(\mu_-' + \nu_-);\quad a_4 = 2\mu_-^2/\mu_0^2 - 1;\quad a_5 = 2\mu_-\nu_-/\mu_0^2;\quad \text{and } \tan\delta = \mu/\nu .$$

The extension of these integrals to the other regions of frequency is quite simple. For $\hbar\omega > \phi$, we must analytically continue ν_+ to $-i(\mu^2+\mu_m^2-\mu_0^2)^{1/2}$ for $\mu > (\mu_0^2-\mu_m^2)^{1/2}$, if $\mu_m < \mu_0$, or for all values of μ if $\mu_m > \mu_0$. On the other hand, when $\mu_m > 1$ (i.e., $\hbar\omega > E_F$) the integrals I_3 and I_5 disappear, while the upper limit of the integral I_2 is replaced by unity. The generalization of these formulas to other regions of space, although straightforward, leads to forms that are cumbersome and not very illuminating. They will not be presented here since the behavior we have analyzed in the text occurs for z and $z' < 0$.

An interesting special case arises in Eqs. (A2)–(A6) on going to the infinite-barrier limit $V_0 \to \infty$. Then $\mu_0 \to \infty$, ν, $\nu_\pm \to \mu_0$, and $a_1 \to -1$, $a_2 \to 0$, $a_3 \to -1$, $a_4 \to -1$, and $a_5 \to 0$. Also the phase shift δ approaches π. An analysis of the integrals appearing in Eqs. (A2)–(A6) *in this limit,* and comparing them with the integrals of Eqs. (5b)–(5f), shows that

$$S^{zz}(0,\omega;\tilde{z},\tilde{z}') \underset{z,z'<0}{\to} S_0^{zz}(0,\omega;\tilde{z}-\tilde{z}') - S_0^{zz}(0,\omega;\tilde{z}+\tilde{z}') + S_{\rm int}^{zz}(0,\omega;\tilde{z},\tilde{z}') , \tag{A7}$$

where the last term on the right is the quantum-mechanical interference term given by ($z > z'$)

$$S_{\rm int}^{zz}(0,\omega;\tilde{z},\tilde{z}') = \left(\frac{\hbar\omega}{2E_F}\right)\int_0^1 d\mu(1-\mu^2)\Big[-\frac{\cos\mu(\tilde{z}-\tilde{z}')\sin\mu_+(\tilde{z}+\tilde{z}') + \sin\mu_+(\tilde{z}-\tilde{z}')\cos\mu(\tilde{z}+\tilde{z}')}{\mu_+}$$
$$+\Theta(\mu_m-\mu)\frac{\cos\mu(\tilde{z}-\tilde{z}')e^{-\mu_-'|\tilde{z}+\tilde{z}'|} - \cos\mu(\tilde{z}+\tilde{z}')e^{-\mu_-'(\tilde{z}-\tilde{z}')}}{\mu_-'}$$
$$+\Theta(\mu-\mu_m)\frac{\cos\mu(\tilde{z}-\tilde{z}')\sin\mu_-(\tilde{z}+\tilde{z}') + \sin\mu_-(\tilde{z}-\tilde{z}')\cos\mu(\tilde{z}+\tilde{z}')}{\mu_-}$$
$$-i\frac{\cos\mu(\tilde{z}-\tilde{z}')\cos\mu_+(\tilde{z}+\tilde{z}') - \cos\mu(\tilde{z}+\tilde{z}')\cos\mu_+(\tilde{z}-\tilde{z}')}{\mu_+}$$
$$+i\Theta(\mu-\mu_m)\frac{\cos\mu(\tilde{z}+\tilde{z}')\cos\mu_-(\tilde{z}-\tilde{z}') - \cos\mu(\tilde{z}-\tilde{z}')\cos\mu_-(\tilde{z}+\tilde{z}')}{\mu_-}\Big] . \tag{A8}$$

The quantum-mechanical interference term drops out and we approach the semiclassical infinite-barrier model[11] as $\hbar\omega \to 0$.

[1]P. Drude, *The Theory of Optics* (Dover, New York, 1959), p. 290.
[2]J. D. E. McIntyre and D. E. Aspnes, Surf. Sci. 24, 417 (1971).
[3]A. B. Pippard, Proc. R. Soc. London Sect. A 191, 385 (1947).
[4]G. E. H. Reuter and E. H. Sondheimer, Proc. R. Soc. London Sect. A 195, 336(1948).
[5]A. B. Pippard, G. E. H. Reuter, and E. H. Sondheimer, Phys. Rev. 73, 920 (1948).
[6]K. L. Kliewer and R. Fuchs, Phys. Rev. 172, 607 (1968).
[7]R. Fuchs and K. L. Kliewer, Phys. Rev. 185, 905 (1969).
[8]N. D. Mermin, Phys. Rev. B 1, 2362 (1970).
[9]J. M. Keller, R. Fuchs, and K. L. Kliewer, Phys. Rev. B 12, 2012 (1975).
[10]K. L. Kliewer, Phys. Rev. B 14, 1412 (1976).
[11]G. Mukhopadhyay and S. Lundqvist, Solid State Commun. 21, 629 (1977); Phys. Scr. 17, 69 (1978).
[12]P. Apell, Phys. Scr. 17, 535 (1978).
[13]P. J. Feibelman, Phys. Rev. B 12, 1319 (1975).
[14]A. Bagchi, Phys. Rev. B 15, 3060 (1977).
[15]J. Anderson, G. W. Rubloff, M. A. Passler, and P. J. Stiles, Phys. Rev. B 10, 2401 (1974).
[16]J. B. Restorff, Ph.D. thesis (University of Maryland, College Park, 1976) (unpublished).
[17]A. M. Brodskii and M. I. Urbakh, Elektrokhimiya 11, 905 (1975) [Sov. Electrochem. 11, 836 (1975)].
[18]A. Bagchi and A. K. Rajagopal, Solid State Commun. 31, 127 (1979). A. Bagchi, R. G. Barrera, and A. K. Rajagopal, Phys. Rev. (to be published).
[19]A. R. Melnyk and M. J. Harrison, Phys. Rev. B 2, 835 (1970).
[20]D. Pines and P. Nozières, *The Theory of Quantum Liquids* (Benjamin, New York, 1966), Vol. I, p. 287.
[21]M. J. Lighthill, *Introduction to Fourier Analysis and Generalized Functions* (Cambridge University, Cambridge, 1960), Chap. 4.
[22]Same point is made in Refs. 11 and 12.
[23]G. Mukhopadhyay and S. Lundqvist, Solid State Commun. 25, 881 (1978).